Biomed Microdevices (2014) 16:673–679
DOI 10.1007/s10544-014-9871-3

A sandwich substrate for ultrasensitive and label-free SERS spectroscopic detection of folic acid / methotrexate

Jing Yang · Xuebin Tan · Wei-Chuan Shih · Mark Ming-Cheng Cheng

Published online: 23 May 2014

Abstract A highly sensitive surface enhanced Raman scattering (SERS) substrate with particle-film sandwich geometry has been developed for the label free detection of folic acid (FA) and methotrexate (MTX). In this sandwich structure, the bottom layer is composed of a copper foil decorated with silver nanoparticles synthesized by the galvanic displacement reaction, and top layer is constituted by silver nanoparticles. The FA and MTX molecules are sandwiched between the silver nanoparticles decorated copper film and the silver nanoparticles. The plasmonic coupling between the two layers of the sandwich structure greatly enhances the SERS spectra of FA and MTX. SERS activity of the substrate was studied and optimized by adjusting the time of galvanic displacement reaction. The SERS spectra of the FA and MTX showed the minimum detection concentration of 100 pM. The identification of methotrexate and folic acid analogs was also carried out by SERS spectra analysis.

Keywords Surface enhanced Raman scattering (SERS) · Folic acid · Methotrexate

1 Introduction

Folic acid (FA) is a pterin-based B vitamin which plays a key role in biosynthetic processes. Folic acid facilitates the transfer of one-carbon units from donor molecules into biosynthetic pathways leading to methionine, purine and pyrimidine biosynthesis (Lucock 2000). In recent studies, FA is also found to be a promising agent for tumor targeting and antitumor drug delivery (Sahu et al. 2010; Wang et al. 2011; Zhang et al. 2010). Methotrexate (MTX) works by blocking some of the side effects of FA. As an analog of FA, MTX is widely used for the treatment of various malignancies, including osteosarcoma, lymphomas, breast cancer, leukemia and autoimmune diseases (Treon and Chabner 1996; Storb et al. 1986; Burak et al. 1998; Bonadonna et al. 1995). In clinical settings, high-dosage methotrexate therapy requires careful monitoring of the drug in serum to ensure minimal toxic effects. In addition, FA deficiency may cause side effects such as mouth sores as well as stomach and liver problems, and these side effects sometimes cause patients to stop taking MTX, which will lead to discontinued treatment (Shea et al. 2013). Patients who are being treated with MTX may be asked to take FA tablets to reduce these unwanted side-effects. FA supplementation has been approved to reduce the toxicity of MTX on blood cells, the gastrointestinal tract and the liver (Prey and Paul 2009). Determining the contents of FA and MTX is critical to medical diagnosis. Various analytical techniques have been used for the detection of FA or MTX, such as UV absorption spectroscopy, electrophoresis combined laser-induced fluorescence detection (Roach et al. 1988) and high-performance liquid chromatography (HPLC). Similarity in appearance as well as physical and chemical properties between FA and MTX makes it difficult to distinguish FA from MTX simultaneously by using the above techniques. Currently, the identification of FA and MTX was realized by mass spectrometry (Hignite and Azarnoff 1978). However, mass spectrometry is relatively time-consuming with low sensitivity.

In recent years, surface enhanced Raman scattering (SERS) spectroscopy has attracted considerable interest in biomolecule detection. As one of the most sensitive analytical techniques for identification of molecular species, SERS has the

Electronic supplementary material The online version of this article (doi:10.1007/s10544-014-9871-3) contains supplementary material, which is available to authorized users.

J. Yang · X. Tan · M. M.-C. Cheng (✉)
Department of Electrical and Computer Engineering, Wayne State University, Detroit, MI, USA
e-mail: mcheng@wayne.edu

W.-C. Shih
Department of Electrical and Computer Engineering, The University of Houston, Houston, TX, USA

potential to monitor and quantify biomolecules down to the single molecule level. In order to improve the limit of detection (LOD) of the SERS signal, recently, the galvanic displacement reaction has received increasing attention as a simple method to synthesize metal nanoparticle decorated substrates for SERS detection (Gutes et al. 2010; Wang et al. 2009; Lai et al. 2011; Betz et al. 2012). In these cases, the metal decorated substrates are the only enhanced media for SERS enhancement; therefore, the local plasmonic coupling between the nanoparticles is restricted to the 2-D domain. Herein, we propose a label free sandwich detection strategy that yields a significant improvement in detection capabilities. We introduce silver nanoparticles onto the silver particle decorated film to further improve the SERS signals of FA and MTX. To evaluate the Raman enhancement of the sandwich substrate, we compared the 3-D sandwich substrate with the bottom silver nanoparticle decorated substrate and pure silver nanoparticles which is a 2-D substrate. The SERS-based sandwich structure has been widely used in immunoassays, in which the Raman reporters with large Raman cross-sections are introduced into the nanoparticles (Song et al. 2009; Guven et al. 2011; Li et al. 2012; Grubisha et al. 2003). Most of the sandwich substrates use "Raman reporters" to label the target agents. In our sandwich structure, there are no "Raman reporters" introduced, so it can achieve sensitive label free detection of biomolecules. Compared with the single substrate, the sandwich SERS substrate enables strong plasmonic coupling between the bottom substrate and the top silver nanoparticles, which provides higher sensitivity.

2 Materials and methods

Folic acid (FA), Methotrexate (MTX), silver nitrate ($AgNO_3$), bovine serum albumin (BSA), and sodium citrate were purchased from sigma-Aldrich. Copper foils were purchased from Alfa Aesar. Water used in the experiments was ultrapure deionized (DI) water with resistance 18.1 $M\Omega \cdot cm^{-1}$.

The silver nanoparticles were synthesized using the citrate-reduction method described by Lee and Meisel (Lee and Meisel 1982). The greenish yellow silver colloids were stored in the dark until used.

A simple way to prepare a uniform substrate with very high SERS activity was developed. The copper foils with natural oxidization were first cut into pieces of 1.5 cm×2.0 cm and washed consecutively with acetone, ethanol and DI water to remove the organic impurities. Then the silver nanoparticles were deposited onto the copper foils by the galvanic displacement reaction. Briefly, the copper foils were immersed in a 1 mM $AgNO_3$ aqueous solution at room temperature. During this process, the silver ions from the solution were reduced by copper atoms on the surfaces of the copper foils. The continuous reduction process leads to the deposition of silver atoms onto copper foil surface, and silver nanoparticles were formed. The density of silver nanoparticles on copper foil was dependent on the reaction time of copper foil in $AgNO_3$ solution. Different reaction time varies from 10 min to 60 min and was carried out to optimize the density of the silver nanoparticles on copper foil. Afterwards, the resultant SERS substrates were rinsed with DI water and dried with a gentle flow of nitrogen.

The SERS spectra were measured at 532 nm excitation using the E-Z Raman spectroscopy system. The Raman scattering light was recorded with a 20× microscope objective. The instrument was calibrated with a signal from a silicon standard at 520 cm^{-1}. FA/MTX in water solution or BSA solution was added into silver nanoparticles with concentrations ranging from 1.0×10^{-6} M to 1.0×10^{-10} M. For SERS measurement, 2 μL of the FA or MTX/Ag complex were dropped onto the two SERS substrates. For each sample, 6 spectra from different positions of the substrate within the droplet were collected to obtain the averaged spectra. All the SERS measurements were performed with a 10 s integration time.

The extinction spectra were collected using a Shimadzu model UV2600 scanning spectrophotometer over the range from 300 nm to 800 nm. The silver nanoparticles were loaded into a 1 cm quartz cell for measurements. The morphology and microstructure of the SERS substrates were obtained using a JSM-6510LVscanning electron microscope (SEM).

3 Results and discussion

Figure 1 shows the schematic diagram of the sandwich substrate. The FA and MTX samples were mixed with silver nanoparticles and then dropped onto the silver nanoparticle decorated copper foil. The FA and MTX molecules would not introduce serious aggregations of silver nanoparticles. As shown in UV-vis spectra of silver nanoparticles and the FA/MTX mixed silver nanoparticles in Figure S1, silver nanoparticles exhibited a surface plasma resonance (SPR) band at 409 nm. There was no significant shift in SPR band after the addition of FA/MTX. A tiny shift of the SPR band (2 nm) was observed due to the change in the dielectric constant of the silver nanoparticles, which can be taken as an indication that the silver nanoparticles did not aggregate.

In previous studies, many researchers have reported detecting sensitive biomolecules via solid SERS substrates (Song et al. 2009; Alvarez-Puebla et al. 2012). Among these substrates, most are based on the self-assembly of silver or gold nanoparticles on glass substrates (Lu et al. 2005; Chumanov et al. 1995). The procedures of manufacturing those substrates are complicated and time-consuming. On the other hand, the substrate based on a galvanic displacement reaction between silver ion and copper is simple. The reaction time determines the density of the silver nanoparticles. To the best of our

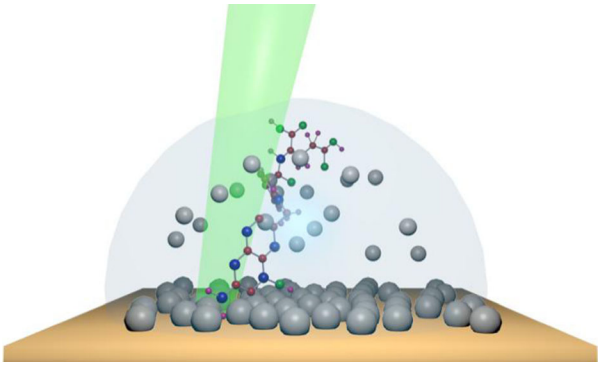

Fig. 1 A schematic view of the sandwich substrate

knowledge, there have been limited studies on SERS intensity dependence on the density of silver nanoparticles by galvanic displacement reaction.

To optimize the SERS enhancement of the SERS substrates, the copper foils were immersed into the $AgNO_3$ solution for different reaction times. Scanning Electron Microscope (SEM) was utilized to characterize the morphology and the density of silver particles on the SERS substrates with different reaction time. As shown in Fig. 2, pure copper foil showed a smooth surface, and the silver particles grew very quickly in the presence of $AgNO_3$ solution. After a 10-min reaction, the copper foil was covered with a few silver nanoparticle clusters. The number and diameter of the silver particles increased with the reaction time as shown in Fig. 2e-f. After 30 min, the silver nanoparticles grown on copper foil had uniform size (100–150 nm) and distribution (Fig. 2g-h). Longer reaction time led to over-sized silver nanoparticles and aggregated silver nanoparticles on copper foil, as shown in Fig. 2i-j. SERS signals are enormously enhanced when the analytes are localized at a hot junction spot between closely-coupled nanoparticles (Qian and Nie 2008; Camden et al. 2008). Abundant "hot spots" were formed at the junctions of the silver nanoparticles, which provides huge SERS enhancement for the substrate. On the other hand, larger nanoparticle aggregates were formed which may block the "hot spots".

To investigate the SERS activity of these silver decorated copper substrates, the SERS performance of FA with silver nanoparticles was measured. As shown in Fig. 2k-l, the spectra of FA at a concentration of 1.0×10^{-6} M from substrates with different reaction times clearly exhibit characteristic peaks of FA molecules at 991 cm^{-1}, 1,201 cm^{-1}, 1,343 cm^{-1}, 1,400 cm^{-1}, 1,502 cm^{-1}, and 1,594 cm^{-1}, respectively. The intensity of the SERS signals increased with the reaction time from 0 min to 30 min. The SERS substrate with a reaction time of 30 min exhibited the maximum intensity of FA SERS signals. From the results, the SERS performances were found consistent with the morphology and the density of silver particles on the SERS substrates as shown in Fig. 2a-j. The low-density substrates lacked effective "hot spots", and the aggregates on high-density substrates may block the "hot spots". Based on these results, the optimized substrate with a reaction time of 30 min was chosen for future SERS detection.

The optimized silver nanoparticle decorated copper foil shows strong SERS enhancement of FA. Moreover, silver nanoparticles were incorporated onto the silver particle decorated film to further improve the SERS signals of FA. To evaluate the Raman enhancement of the sandwich substrate, we compared the SERS signals of FA from the sandwich substrate with the signals from bottom silver nanoparticle decorated substrate and pure silver nanoparticles. In Fig. 3, we observed that the sandwich structure exhibited stronger Raman enhancing ability compared to the pure silver nanoparticle and the silver nanoparticles decorated copper foil substrate. The SERS intensity of the FA on sandwich substrates was more than 10 times higher than the intensities of FA on the bottom silver substrate and silver nanoparticles. The results indicate the strong plasmonic coupling between the bottom substrate and the top silver nanoparticles, which will greatly increase the SERS intensity (Halas et al. 2011).

FA and MTX are analogues with very similar chemical structures. It is very challenging to identify the two molecules simultaneously. Thanks to the unique signatures of SERS spectra, the two analogues can be identified using SERS spectroscopy. The SERS spectra of FA and MTX were recorded under identical conditions as shown in Fig. 4a. The discrimination of these two molecules is clearly demonstrated, which would be difficult to distinguish by other methods, such as fluorescent spectroscopy and absorption spectroscopy.

The characteristic Raman bands of FA and MTX were confirmed according to previous studies (Stokes et al. 2008; Ren et al. 2011; Ozaki et al. 1981; Saperstein et al. 1978; Durig et al. 1980). As shown in Fig. 4a, FA and MTX had some Raman bands in common, such as the band at 1,201 cm^{-1} and the most prominent band at 1,594 cm^{-1}. Meanwhile, FA and MTX exhibited plenty of different Raman characteristic bands. These characteristic peaks provided the information of the molecules that could be utilized to distinguish FA from MTX. MTX showed its characteristic Raman bands at 715 cm^{-1}, 974 cm^{-1}, 1,275 cm^{-1}, 1,360 cm^{-1}, 1,528 cm^{-1}, and 1,563 cm^{-1}, while FA exhibited its characteristic Raman bands at 693 cm^{-1}, 991 cm^{-1}, 1,181 cm^{-1}, 1,343 cm^{-1}, 1,400 cm^{-1}, and 1,502 cm^{-1}. Considering the peak intensity and position, the characteristic Raman bands at 1,502 cm^{-1} and 1,563 cm^{-1} were chosen as the Raman label of FA and MTX, respectively.

To validate the identification ability of SERS, FA (1.0×10^{-6} M) and MTX (1.0×10^{-6} M) were mixed at different molar ratios. The SERS spectra of these mixture solutions are shown in Fig. 4b. The result demonstrated that FA exhibited a stronger SERS signal than MTX. When FA and MTX were mixed at a mole ratio of 1:1, the SERS spectra of the mixture looked like the spectra of FA. It was observed that when the ratio of FA: MTX was increased to 1:10, the bands of MTX at 974 cm^{-1}, 1,360 cm^{-1} and 1,563 cm^{-1} started to

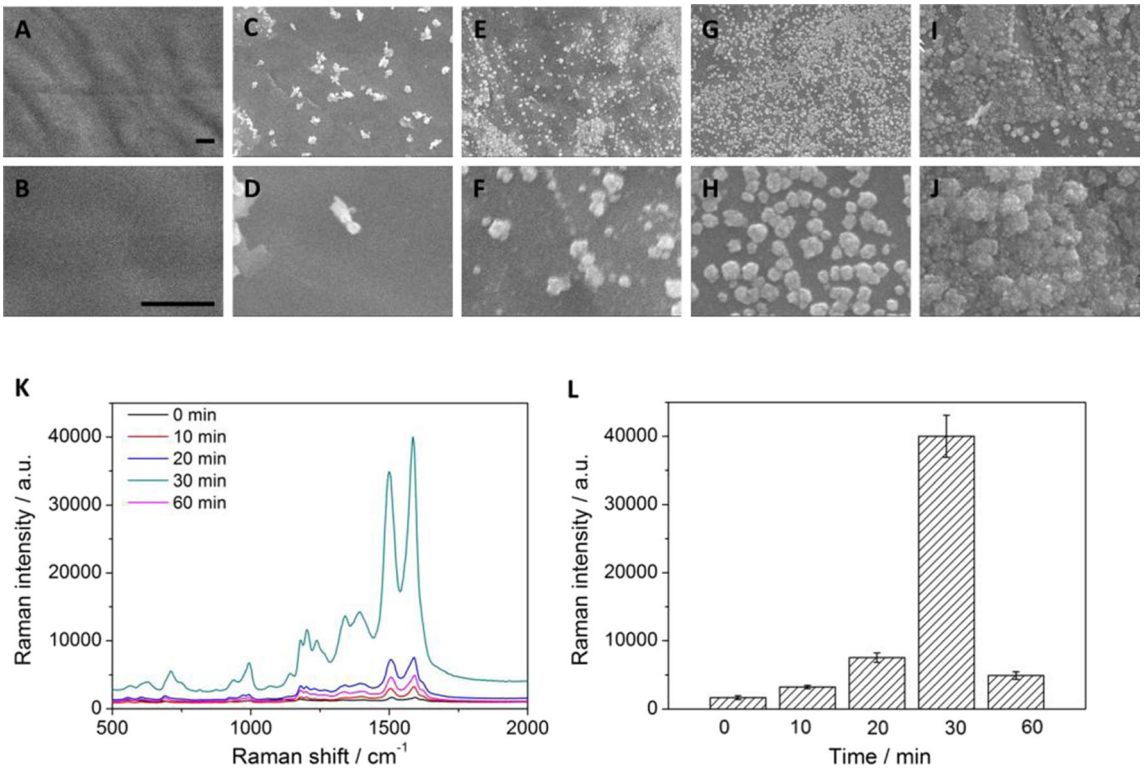

Fig. 2 SEM images of SERS substrates with different reaction time: (**a**, **b**) 0 min; (**c**, **d**) 10 min, (**e**, **f**) 20 min, (**g**, **h**) 30 min and (**i**, **j**) 60 min. The scale bars are 1 μm. The SERS spectra of FA at the concentration of 1.0×10–6 M (**k**) on the above substrates and (**l**) the corresponding SERS intensities

appear. As the increase of MTX, the SERS intensities of the bands at 974 cm^{-1}, 1,360 cm^{-1} and 1,563 cm^{-1} kept increasing. The characteristic bands of MTX at 974 cm^{-1}, 1,360 cm^{-1} and 1,563 cm^{-1} can be used as the characteristic bands of MTX.

The SERS sensitivity of the sandwich substrate was quantified. SERS substrate with a reaction time of 30 min with $AgNO_3$ solution was exposed to different concentrations of FA, and their SERS spectra were measured as shown in Fig. 5a-b. The concentration of FA in water solution was tested from 1.0 μM to 100 pM. The detection limit of the SERS substrate for FA was determined 100 pM. As the concentrations of FA decreased, the SERS signals of FA decreased. The LOD of FA was 100 pM. The SERS substrates also showed the sensitive SERS sensing ability of MTX. As shown in Fig. 5c-d, the SERS signals of MTX decreased with the decrease of MTX and the LOD of MTX was 100 pM. To apply the SERS substrate to more practical applications, we tested the FA in PBS buffer with 1 % BSA. The LOD of FA in BSA solution was 1 nM (Figure S2). The reduced SERS sensitivity was probably due to the aggregation of silver nanoparticles in the presence of ions in buffer, including chloride and phosphate ions.

Previous studies showed successful applications of SERS-based FA sensing. Graham et al. developed a SERS-based FA detection by using ethylene-diaminetetraacetic acid (EDTA)

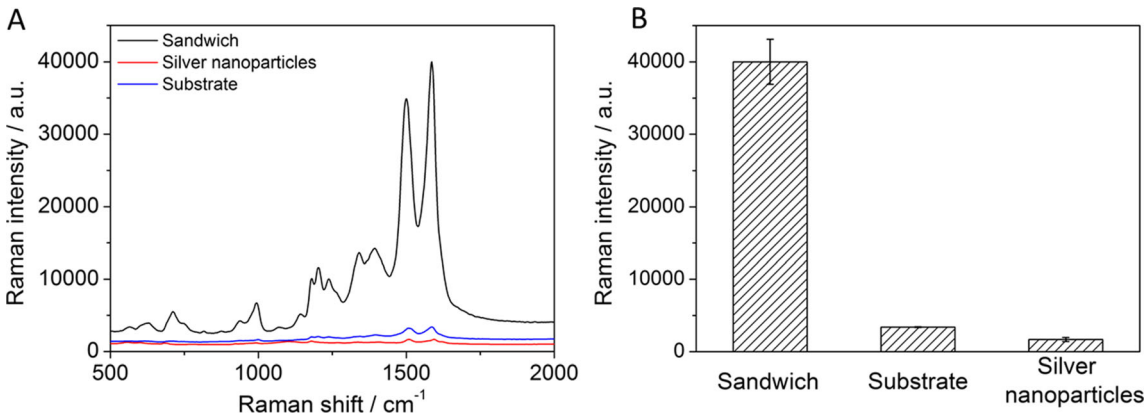

Fig. 3 SERS spectra (**a**) and the corresponding intensities (**b**) of FA on different substrates

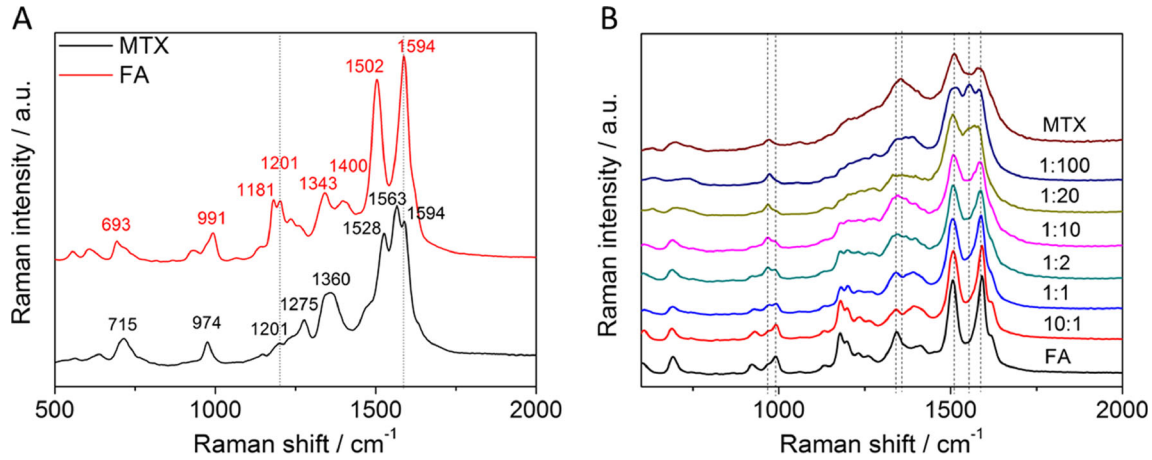

Fig. 4 Characteristic Raman peaks of FA and MTX (**a**); SERS spectra of FA and MTX as well as mixtures of FA and MTX with different mole ratios (**b**)

reduced silver nanoparticles, and the limit of detection (LOD) was 18 nM (Stokes et al. 2008). Ren et al. reported a self-assemble graphene oxide/Ag hybrid substrate for ultrasensitive SERS detection of FA in both water and human serum with a minimum-detected concentration up to 9 nM (Ren et al. 2011). These methods suffer from high LOD or a complicated fabrication process. A sensitive SERS substrate with a simple fabrication process is still a challenge. More important, although there is an urgent demand for detecting FA and MTX simultaneously, to our knowledge, however, SERS-based MTX detection has not yet been reported. Our previous study proved that SERS has significant advantages with multiplex

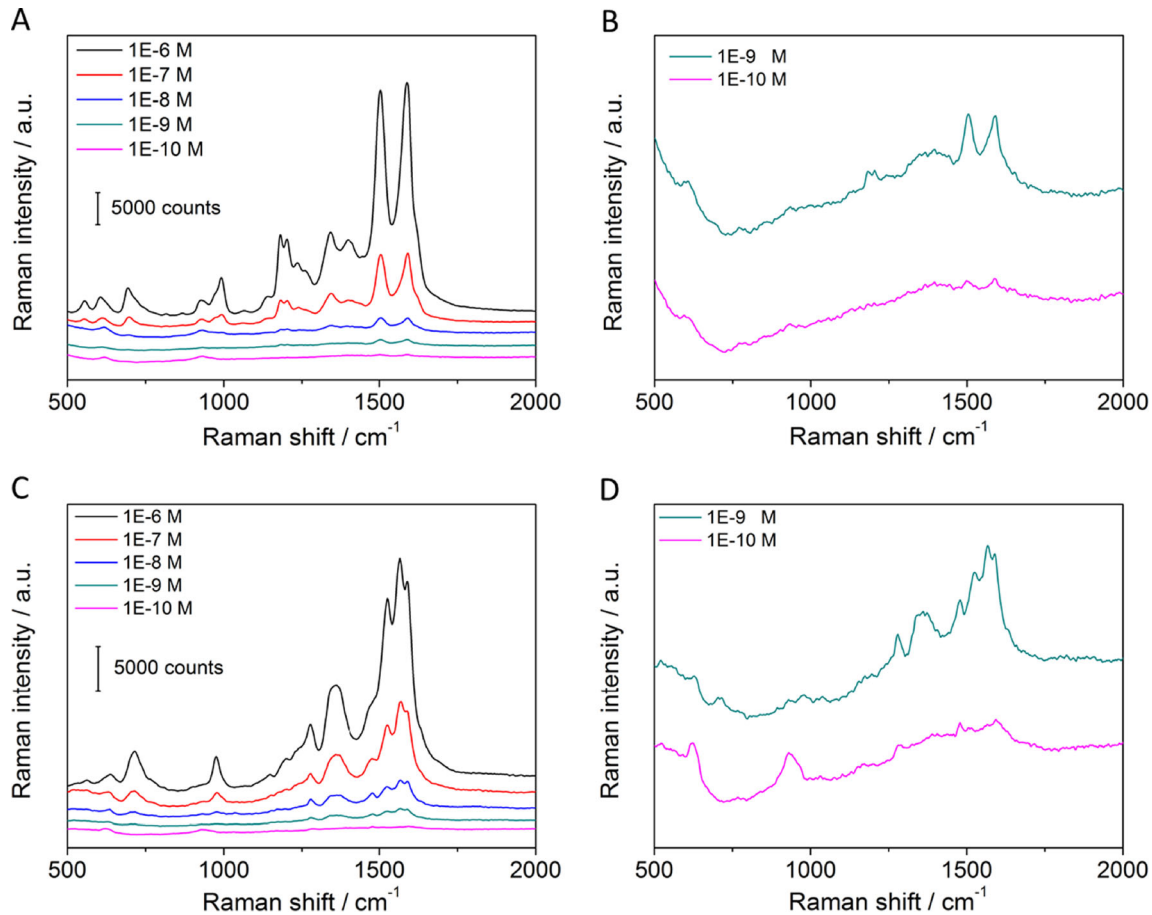

Fig. 5 SERS spectra of FA (**a**) and MTX (**c**) with different concentrations on sandwich substrate, **b** and **d** are the zoom out figures of FA and MTX at low concentrations, respectively

drug detection due to the narrow emission bands (Yang et al. 2012). The SERS spectra of both FA and MTX showed the minimum detection concentration of 100 pM. To the best of our knowledge, it is the most sensitive detection of FA and MTX based on SERS.

In this paper we developed a simple and high-efficiency sandwich SERS substrate for ultra-sensitive FA and MTX sensing. The sandwich structure takes full advantage of the plasmonic coupling between the top silver nanoparticles and the bottom substrates. The morphology of the sandwich substrates is optimized to obtain the greatest SERS performance. Our substrates have several advantages, including (1) it is very easy to synthesize at a low cost, (2) the size of the silver nanoparticles can be controlled by reaction time, and (3) the "hotspots" form aggregates that can provide high Raman enhancement. The LOD of FA and MTX can reach as low as 100 pM, which is the lowest LOD when compared to previous studies. The SERS spectra of FA, MTX and their mixtures with different mole ratios exhibit the potential to identify MTX from its analog, FA.

Acknowledgments This work was supported by NSF CAREER Award (1055932) MRI Award (1229635) and Wayne State University. We thank Dr. Da Deng for the help of UV-vis absorption spectroscopy measurement.

References

R.A. Alvarez-Puebla, E.R. Zubarev, N.A. Kotov, L.M. Liz-Marzan, Self-assembled nanorod supercrystals for ultrasensitive SERS diagnostics. Nano Today **7**, 6–9 (2012)

J.F. Betz, Y. Cheng, G.W. Rubloff, Direct SERS detection of contaminants in a complex mixture: rapid, single step screening for melamine in liquid infant formula. Analyst **137**, 826–828 (2012)

G. Bonadonna, P. Valagussa, A. Moliterni, M. Zambetti, C. Brambilla, Cyclophosphamide, methotrexate, and fluorouracil in node-positive breast-cancer - the results of 20 years of follow-up. New Engl J Med **332**, 901–906 (1995)

K.W. Burak, S.J. Urbanski, M.G. Swain, Successful treatment of refractory type 1 autoimmune hepatitis with methotrexate. J. Hepatol. **29**, 990–993 (1998)

J.P. Camden, J.A. Dieringer, Y.M. Wang, D.J. Masiello, L.D. Marks, G.C. Schatz, R.P. Van Duyne, Probing the structure of single-molecule surface-enhanced Raman scattering hot spots. J. Am. Chem. Soc. **130**, 12616 (2008)

G. Chumanov, K. Sokolov, B.W. Gregory, T.M. Cotton, Colloidal metal-films as a substrate for surface-enhanced spectroscopy. J. Phys. Chem. **99**, 9466–9471 (1995)

J.R. Durig, R.B. Dunlap, D.J. Gerson, Conformational study of methotrexate binding to L-Casei dihydrofolate-reductase by laser Raman-spectroscopy. J. Raman Spectrosc. **9**, 266–272 (1980)

D.S. Grubisha, R.J. Lipert, H.Y. Park, J. Driskell, M.D. Porter, Femtomolar detection of prostate-specific antigen: an immunoassay based on surface-enhanced Raman scattering and immunogold labels. Anal. Chem. **75**, 5936–5943 (2003)

A. Gutes, C. Carraro, R. Maboudian, Silver dendrites from galvanic displacement on commercial aluminum foil as an effective sers substrate. J. Am. Chem. Soc. **132**, 1476 (2010)

B. Guven, N. Basaran-Akgul, E. Temur, U. Tamer, I.H. Boyaci, SERS-based sandwich immunoassay using antibody coated magnetic nanoparticles for Escherichia coli enumeration. Analyst **136**, 740–748 (2011)

N.J. Halas, S. Lal, W.S. Chang, S. Link, P. Nordlander, Plasmons in strongly coupled metallic nanostructures. Chem. Rev. **111**, 3913–3961 (2011)

C.E. Hignite, D.L. Azarnoff, Identification of methotrexate and folic acid analogs by mass spectrometry. Biol Mass Spectrome **5**, 161–163 (1978)

Y.C. Lai, W.X. Pan, D.J. Zhang, J.H. Zhan, Silver nanoplates prepared by modified galvanic displacement for surface-enhanced Raman spectroscopy. Nanoscale **3**, 2134–2137 (2011)

P.C. Lee, D. Meisel, Adsorption and surface-enhanced Raman of dyes on silver and gold sols. J. Phys. Chem. **86**, 3391–3395 (1982)

J.M. Li, C. Wei, W.F. Ma, Q. An, J. Guo, J. Hu, C.C. Wang, Multiplexed SERS detection of DNA targets in a sandwich-hybridization assay using SERS-encoded core-shell nanospheres. J. Mater. Chem. **22**, 12100–12106 (2012)

Y. Lu, G.L. Liu, L.P. Lee, High-density silver nanoparticle film with temperature-controllable interparticle spacing for a tunable surface enhanced Raman scattering substrate. Nano Lett. **5**, 5–9 (2005)

M. Lucock, Folic acid: nutritional biochemistry, molecular biology, and role in disease processes. Mol. Genet. Metab. **71**, 121–138 (2000)

Y. Ozaki, R.W. King, P.R. Carey, Methotrexate and folate binding to dihydrofolate-reductase - separate characterization of the pteridine and para-aminobenzoyl binding-sites by resonance Raman-spectroscopy. Biochemistry-Us **20**, 3219–3225 (1981)

S. Prey, C. Paul, Effect of folic or folinic acid supplementation on methotrexate-associated safety and efficacy in inflammatory disease: a systematic review. Brit J Dermatol **160**, 622–628 (2009)

X.M. Qian, S.M. Nie, Single-molecule and single-nanoparticle SERS: from fundamental mechanisms to biomedical applications. Chem. Soc. Rev. **37**, 912–920 (2008)

W. Ren, Y.X. Fang, E.K. Wang, A binary functional substrate for enrichment and ultrasensitive SERS spectroscopic detection of folic acid using graphene oxide/ag nanoparticle hybrids. ACS Nano **5**, 6425–6433 (2011)

M.C. Roach, P. Gozel, R.N. Zare, Determination of methotrexate and its major metabolite, 7-hydroxymethotrexate, using capillary zone electrophoresis and laser-induced fluorescence detection. J Chromatogr-Biomed **426**, 129–140 (1988)

S.K. Sahu, S.K. Mallick, S. Santra, T.K. Maiti, S.K. Ghosh, P. Pramanik, In vitro evaluation of folic acid modified carboxymethyl chitosan nanoparticles loaded with doxorubicin for targeted delivery. J Mater Sci-Mater M **21**, 1587–1597 (2010)

D.D. Saperstein, A.J. Rein, M. Poe, M.F. Leahy, Binding of Methotrexate to Escherichia-Coli Dihydrofolate-Reductase as Measured by Visible and Ultraviolet Resonance Raman-Spectroscopy. J. Am. Chem. Soc. **100**, 4296–4300 (1978)

B. Shea, M.V. Swinden, E.T. Ghogomu, Z. Ortiz, W. Katchamart, T. Rader, C. Bombardier, G.A. Wells, P. Tugwell, Folic acid and folinic acid for reducing side effects in patients receiving methotrexate for rheumatoid arthritis. Cochrane Db Syst Rev **5**. (2013). doi:10.1002/14651858.CD000951.pub2

C.Y. Song, Z.Y. Wang, R.H. Zhang, J. Yang, X.B. Tan, Y.P. Cui, Highly sensitive immunoassay based on Raman reporter-labeled immuno-Au aggregates and SERS-active immune substrate. Biosens. Bioelectron. **25**, 826–831 (2009)

R.J. Stokes, E. McBride, C.G. Wilson, J.M. Girkin, W.E. Smith, D. Graham, Surface-enhanced Raman scattering spectroscopy as a sensitive and selective technique for the detection of folic acid in water and human serum. Appl. Spectrosc. **62**, 371–376 (2008)

R. Storb, H.J. Deeg, J. Whitehead, F. Appelbaum, P. Beatty, W. Bensinger, C.D. Buckner, R. Clift, K. Doney, V. Farewell, J. Hansen, R. Hill, L. Lum, P. Martin, R. Mcguffin, J. Sanders, P.

Stewart, K. Sullivan, R. Witherspoon, G. Yee, E.D. Thomas, Methotrexate and cyclosporine compared with cyclosporine alone for prophylaxis of acute graft versus host-disease after marrow transplantation for leukemia. New Engl J Med **314**, 729–735 (1986)

S.P. Treon, B.A. Chabner, Concepts in use of high-dose methotrexate therapy. Clin. Chem. **42**, 1322–1329 (1996)

Y. Wang, M. Becker, L. Wang, J.Q. Liu, R. Scholz, J. Peng, U. Gosele, S. Christiansen, D.H. Kim, M. Steinhart, Nanostructured gold films for SERS by block copolymer-templated galvanic displacement reactions. Nano Lett. **9**, 2384–2389 (2009)

Z.Y. Wang, S.F. Zong, J. Yang, J. Li, Y.P. Cui, Dual-mode probe based on mesoporous silica coated gold nanorods for targeting cancer cells. Biosens. Bioelectron. **26**, 2883–2889 (2011)

J. Yang, Y.P. Cui, S.F. Zong, R.H. Zhang, C.Y. Song, Z.Y. Wang, Tracking multiplex drugs and their dynamics in living cells using the label-free surface-enhanced Raman scattering technique. Mol Pharmaceut **9**, 842–849 (2012)

Z.W. Zhang, J. Jia, Y.Q. Lai, Y.Y. Ma, J. Weng, L.P. Sun, Conjugating folic acid to gold nanoparticles through glutathione for targeting and detecting cancer cells. Bioorgan Med Chem **18**, 5528–5534 (2010)